NMR study of lineshifts and relaxation rates of the one-dimensional antiferromagnet LiCuVO4

Christian Kegler, Norbert Büttgen, Hans-Albrecht Krug von Nidda, Alois Loidl, R. Nath, A. V. Mahajan, A. V. Prokofiev, W. Aßmus

NMR study of lineshifts and relaxation rates of the one-dimensional antiferromagnet LiCuVO$_4$

C. Kegler,* N. Büttgen, H.-A. Krug von Nidda, and A. Loidl

Experimentalphysik V, Elektronische Korrelationen und Magnetismus, Institut für Physik, Universität Augsburg,
D-86135 Augsburg, Germany

R. Nath and A. V. Mahajan

Department of Physics, IIT Bombay, Powai Mumbai 400 076, India

A. V. Prokofiev and W. Aßmus

Johann Wolfgang Goethe-Universität Frankfurt, Robert-Mayer-Str. 2-4, D - 60325 Frankfurt am Main, Germany

NMR measurements were performed on single-crystalline samples of the one-dimensional Heisenberg antiferromagnet (1D HAF) LiCuVO$_4$. We investigated ^{7}Li and ^{51}V NMR spectra, deduced the respective lineshifts $K(T)$, spin-lattice relaxation rates $1/T_1$, and spin-spin relaxation rates $1/T_2$ and $1/T_{2G}$. The results are compared to theoretical predictions for the relaxation rates $1/T_1(T)$ and $1/T_{2G}(T)$ deduced from the dynamic susceptibility $\chi(\mathbf{q}, \omega)$ of a 1D HAF spin chain as proposed by Sachdev [Phys. Rev. B **50**, 13006 (1994)]. We document a correspondence between the anisotropic relaxation rates derived from electron paramagnetic resonance linewidth $\Delta H(T)$ and nuclear magnetic resonance $1/T_1(T)$, respectively, the former being well described in the framework of symmetric anisotropic exchange interactions for LiCuVO$_4$ by Krug von Nidda *et al.* [Phys. Rev. B **65**, 134445 (2002)].

I. INTRODUCTION

One-dimensional magnetic (1D) systems have gained considerable interest over the past three decades. From a theoretical point of view 1D magnetic systems are the simplest realization of correlated electron systems and have therefore been studied theoretically intensively.[1] Especially, stimulated by the discovery of 1D behavior in CuGeO$_3$ as the first inorganic 1D compound by Hase *et al.* in 1993,[2] the study of 1D Heisenberg antiferromagnets (1D HAF) moved into the focus of the scientific community again. The low-dimensional nature of the compounds has interesting consequences on the wave vector $\mathbf{q}$ and frequency ω dependent electron dynamic susceptibility $\chi(\mathbf{q}, \omega)$, a quantity closely linked to the spin-lattice $1/T_1$ and spin-spin $1/T_2$ relaxation rates of nuclear magnetic resonance (NMR). In the limit $T = 0$ the rate $1/T_1$ was first calculated by Ehrenfreund *et al.*[3] in 1973.

Later, a large share of the interest in 1D systems stemmed from the investigation of high-T_c superconductors (HTS) as the physics in these compounds appears closely linked to the magnetism of the hole-doped 2D CuO$_2$ planes. A possible approach towards the understanding of superconductivity in HTS is to study systems with even lower dimensionality: namely, spin chains. NMR, being a microscopic probe, offers a possibility to study the dynamic electronic susceptibility $\chi(\mathbf{q}, \omega)$ as well as the static electronic susceptibility via the NMR lineshift at the site of the probing nucleus. Models for the temperature dependence of the dynamic susceptibility $\chi(\mathbf{q}, \omega)$ of a 1D spin chain were motivated by models for 2D spin systems in the HTS by Millis *et al.*[4] Sachdev expressed $\chi(\mathbf{q}, \omega)$ in terms of the NMR relaxation rates $1/T_1$ in connection with a Gaussian spin-spin relaxation rate $1/T_{2G}$ and

made predictions for their temperature dependence.[5] His model was very successfully applied to Sr$_2$CuO$_3$, describing the behavior of the spin-lattice relaxation rate $1/T_1(T)$ and the spin-spin relaxation rate $1/T_{2G}(T)$ which result from a Gaussian decay of the transverse magnetization. Sr$_2$CuO$_3$ was reported by other authors[6,7] as a prototypical 1D system with intrachain nearest-neighbor exchange coupling constant of $J/k_B \approx 2200$ K along the chain.[8]

Whereas considerable theoretical work pertaining to the magnetic properties of 1D HAF chains with $S = 1/2$ exists,[1] there are not very many actual realizations of 1D HAFs in nature. In this work, we present results of NMR and electron paramagnetic (EPR) studies of single crystals of LiCuVO$_4$. A broad range of properties of polycrystalline LiCuVO$_4$ have been studied such as structure,[9,10] susceptibility,[11,12] specific heat,[13,14] electrochemical properties,[15] and properties using resonance methods such as NMR and EPR.[16–20] This material gained some interest for its prospective use in rechargeable batteries[15] which are considered important for various applications. As single-crystalline material became available,[21] its properties have been studied by investigating the temperature T dependence of the magnetic susceptibility $\chi(T)$, magnetic structure in the ordered state using neutron diffraction[22] in combination with band-structure calculations,[23] EPR,[17] heat transport, and thermal conductivity[24,25] as well as lattice dynamics by infrared spectroscopy.[26]

Compared to Sr$_2$CuO$_3$, LiCuVO$_4$ has a much lower exchange coupling constant $J/k_B \approx 42$ K and its properties seem prototypical for a class of 1D HAFs together with CuGeO$_3$ and newly reported phosphate compounds.[27]

II. EXPERIMENTAL DETAILS

LiCuVO$_4$ crystallizes in the inverse spinel structure AB_2O_4, with an orthorhombic distortion due to a cooperative Jahn-Teller effect induced by the Cu^{2+} ions (configuration $3d^9$). LiCuVO$_4$ belongs to the space group *Imma* with lattice constants $a = 5.6599(3)$ Å, $b = 5.8108(3)$ Å, and $c = 8.7595(4)$ Å.[10,18] The crystal structure suggests one-dimensional behavior in this compound as Li$^+$ and Cu^{2+} ion form chains pointing along the crystallographic a and b directions, respectively.[10,11,18] The preparation of our single-crystalline samples (dimensions approximately $3 \times 2 \times 5$ mm^3) starting from polycrystalline samples has been described earlier by Prokofiev *et al.*[21] Our NMR measurements were conducted for ^{7}Li and ^{51}V nuclei using a phase-coherent spectrometer with a flow cryostat for temperatures down to 1.8 K. We failed to observe a signal of ^{65,63}Cu nuclei, as the observation of the NMR of a paramagnetic ion is prevented due to large on-site hyperfine interactions resulting in fast relaxation of the nuclear magnetization.[28] The NMR spectra were obtained by recording the echo area as a function of the external field at fixed rf transmitter frequency. To irradiate the nuclei we used a conventional spin-echo sequence of a $\pi/2$ (pulse width τ_A) and a π pulse (pulse width τ_B) separated by a time interval τ_{AB}.

III. EXPERIMENTAL RESULTS

A. ^{7}Li spectra and lineshift $K(T)$

^{7}Li spectra ($I = 3/2$, gyromagnetic ratio $^7\gamma/2\pi = 16.5466$ MHz/T) were collected in a temperature range from 1.5 K to 135 K, using pulses of $\tau_A = 17$ μs and $\tau_B = 34$ μs, respectively, and $\tau_{AB} = 50$ μs. All ^{7}Li spectra were measured against LiCl as the diamagnetic reference with lineshift $^7K = 0$. From the measured spectra we deduced the lineshift as

$$K(T) = \frac{H_{ref} - H_{exp}}{H_{exp}} = \frac{A_{hf}}{N_A \mu_B} \chi_{bulk}(T), \quad (1)$$

where H_{exp} and H_{ref} denote the magnetic field of the resonance line in LiCuVO$_4$ and the reference compound LiCl, respectively, A$_{hf}$ stands for the hyperfine constant and χ_{bulk} for the spin part of the molar magnetic susceptibility of LiCuVO$_4$, N_A is Avogadro's number, and μ_B a Bohr magneton. Figure 1 shows a selection of ^{7}Li spectra in the left column for the single crystal irradiated at a radio frequency of 93.2 MHz and temperatures 14 K, 44 K, and 77 K.

The spectra for the applied magnetic field H parallel to the crystallographic b axis ($H \| b$, solid line) exhibit a line with positive lineshift $K(T)$, which considerably broadens towards lower temperatures. This broadening is attributed to an evolving distribution of hyperfine fields at the nuclear sites approaching the transition into a long-range-ordered state of the electronic system at a $T_N = 1.3$ K.[16,18,20] At higher H, there is a second line with negative lineshift $K(T)$. Measurements at lower applied fields (46.6 MHz, not shown) demonstrate that the splitting of both lines decreases, excluding it from being quadrupolar in origin. We suggest that this sec-
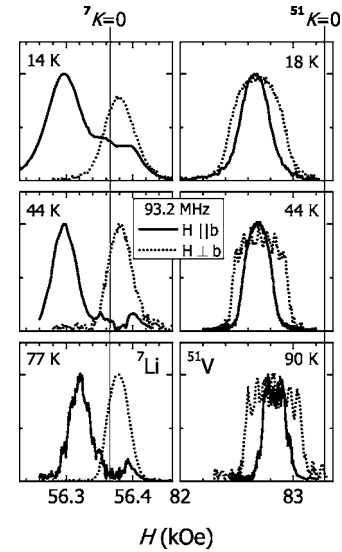

FIG. 1. Temperature dependence of the NMR spectra of single-crystalline LiCuVO$_4$ for ^{7}Li and ^{51}V on the left and right columns, respectively, at 93.2 MHz. Solid and dotted lines depict an orientation of the crystal with $H \| b$ and $H \perp b$, respectively.

ond line stems from a small amount of Cu^{2+} ions occupying Li$^+$ positions within the Li$^+$ chains, changing the magnetic surrounding for the probing ^{7}Li nuclei next to these magnetic Cu^{2+} defects considerably. From fitting the two ^{7}Li lines to Gaussians we obtain that the ratio of relative intensities of the two lines is 0.1 at elevated temperatures. According to our interpretation of Cu^{2+} ions occupying sites within the Li$^+$ chains, each of these copper ions affect the two neighboring lithium sites. Therefore, a nuclei concentration of 0.05 of the positively shifted line is enough to account for the observed second line with negative shift. It has to be clearly stated that a more precise estimation of the relative intensities also at lower temperatures has to include the correction due to the initial magnetizations M_0 of the spin-spin relaxation measurements at these different lines. After rotating the single crystal into an orientation $H \perp b$ with the Cu^{2+} chains running perpendicular to the magnetic field only a single line is resolved for all temperatures showing a negative, but in absolute numbers a smaller lineshift $K(T)$ than for $H \| b$. Figure 2(A) and 2(B) show the shift of the ^{7}Li line for the orientation $H \| b$ and $H \perp b$, respectively. For both orientations the lineshift $K(T)$ nicely follows the Bonner-Fisher-type behavior[29] for the bulk susceptibility $\chi_{bulk}(T)$ of an antiferromagnetic spin chain as indicated by the solid line. This line is a fit using the rational function given by Estes *et al.*[30] The coupling constants J_{NMR}/k_B deduced from these fits are summarized in Table I for ^{7}Li NMR for comparison with the respective values of the bulk susceptibility. We note that the strong anisotropy of the ^{7}Li lineshift seems to be intimately connected with the crystallographic arrangement of the Li$^+$ ions on nonmagnetic chains. The strong anisotropy of the ^{7}Li lineshift is consequently also reflected in the orientational dependence of the hyperfine coupling as it can be deduced from Jaccarino-Clogston plots[31,32] where the measured lineshift $K(T)$ is plotted versus the bulk susceptibility $\chi_{bulk}(T)$ with temperature T being an implicit parameter according to
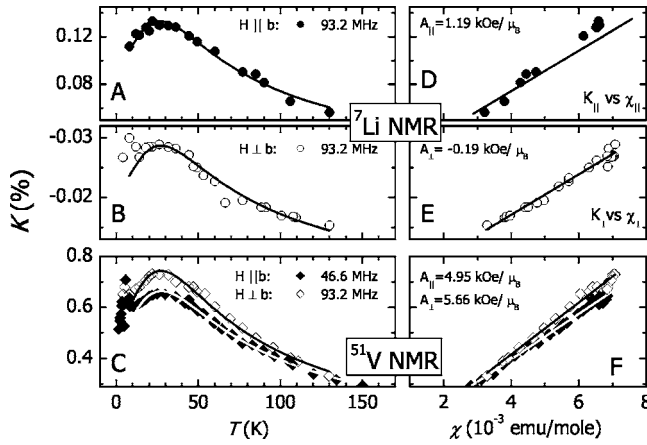
FIG. 2. Left column: NMR lineshifts $K(T)$ vs T in single-crystalline LiCuVO$_4$ for ^{7}Li (A), (B) and ^{51}V NMR (C), measured for different orientations of the crystal with respect to H. Right column: plots of $K(T)$ vs $\chi(T)$ with T as implicit parameter for ^{7}Li (D), (E) and ^{51}V (F) yielding the hyperfine coupling constants $A_\parallel$ and $A_\perp$.

Eq. (1). Such plots are shown in Figs. 2(D) and 2(E) for which the slope gives the hyperfine coupling constants $A_\parallel$ = 1.19 kOe/μ_B and $A_\perp$ = −0.19 kOe/μ_B, respectively.

B. ^{51}V spectra and lineshift $K(T)$

For the ^{51}V-NMR experiments ($I=7/2$, gyromagnetic ratio $^{51}\gamma/2\pi=11.193$ MHz/T) the pulse lengths used in the spin-echo sequence were $\tau_A=2$ μs and $\tau_B=4$ μs with a pulse separation of $\tau_{AB}=45$ μs for the orientation of $H\|b$ of the crystal at 93.2 MHz. In the orientation $H\perp b$ the pulse lengths were $\tau_A=5$ μs and $\tau_B=10$ μs and a pulse separation of $\tau_{AB}=50$ μs. ^{51}V spectra are shown in the right column of Fig. 1 for temperatures 18 K, 44 K, and 90 K. Also shown is the position of the reference VOCl$_3$ for $^{51}K=0$. Spectra for $H\|b$ are depicted as solid lines whereas those for $H\perp b$ are indicated by dotted lines. The typical structure for an $I=7/2$ system perturbed by a quadrupolar interaction showing seven distinct lines can be resolved in both orientations at sufficiently high temperatures. The splitting of the line shows a strong orientational dependence as it is twice as large for $H\perp b$ as it is for $H\|b$. This behavior is expected in the case

TABLE I. Summary of the values of the exchange coupling constants J as deduced from Bonner-Fisher fits to $K(T)$ for ^{7}Li and ^{51}V NMR in both orientations of the crystal $H\|b$ and $H\perp b$ at 93.2 MHz. Additionally, values for J_{bulk} deduced from superconducting quantum interference device (SQUID) measurements on the single crystal are given for comparison.

	Orientation of the crystal	
	$H\|b$	$H\perp b$
^{7}Li J_{NMR}/k_B(K)	40.9±1.3	46.6±3
^{51}V J_{NMR}/k_B(K)	43.8±1	43.6±1
J_{bulk}/k_B(K)	44.3±0.3	44.0±0.3

of an axial symmetric electric field gradient (EFG) at the probing ^{51}V site when rotating the symmetry axis of the crystal by 90° with respect to the direction of H. For both orientations one finds again a considerable broadening of the line towards lower temperatures approaching the long-range ordering at T_N. With lower temperature the structure in the line shape gets smeared out leading to a broad single resonance line.

The center of gravity for the ^{51}V resonance-line pattern remains mostly unaffected by the rotation of the crystal. The lineshift $K(T)$ deduced from the central transition of the ^{51}V resonance-line pattern is shown in Fig. 2(C). In both orientations one finds a behavior typical of one-dimensional systems showing a broad maximum around $T\approx 28$ K that can be nicely described by the Bonner-Fisher model as documented by a corresponding fit[30] depicted as solid black and grey lines for $H\|b$ and $H\perp b$, respectively. The deduced exchange coupling constants J_{NMR}/k_B are given in Table I and again confirm the values from the bulk susceptibility. The upturn of the measured lineshift $K(T)$ for $T<10$ K followed by a sharp peak at $T\approx 3$ K reflects the transition into the 3D magnetic order of the electronic system. The hyperfine constants for ^{51}V are deduced from Fig. 2(F) and reflect, with $A_\parallel$ =4.95 kOe/μ_B and $A_\perp$=5.66 kOe/μ_B for $H\|b$ and $H\perp b$, respectively, the nearly isotropic behavior at the ^{51}V site.

In summary, ^{7}Li and ^{51}V NMR lineshifts track the one-dimensional magnetic behavior of the Cu^{2+} chains. The lineshift measurements $K(T)$ revealed that the temperature dependence of the local susceptibility could be described with the Bonner-Fisher model. For both nuclei, the resulting value of the exchange coupling constant J/k_B of Cu^{2+} ions exhibited almost no dependence on the orientation of the crystal with respect to the applied magnetic field. The absolute values of the lineshift K, however, showed strongly different behavior for both nuclei: The lineshift values in case of ^{7}Li were found to be strongly anisotropic, even changing the sign when the crystal was rotated by 90°, with respect to H, whereas the lineshift values in case of ^{51}V were found to show only minor anisotropy yielding similar hyperfine coupling constants $A_\parallel$ and $A_\perp$ in contrast to the hyperfine coupling of the ^{7}Li nuclei.

C. ^{7}Li and ^{51}V spin-lattice relaxation T_1

The relaxation of the longitudinal nuclear magnetization $M_z(\tau)$ for ^{7}Li and ^{51}V was measured using a spin-echo recovery sequence consisting of a π pulse followed, after a variable delay τ_{BC}, by a standard spin-echo sequence with pulse separation τ_{AB}. The pulse parameters of the spin-echo sequence used for measurements in the orientation $H\|b$ (46.6 and 93.2 MHz) for both nuclei were $\tau_A=17$ μs and τ_B =34 μs with a pulse separation $\tau_{AB}=50$ μs. The same parameters were used for ^{7}Li in the orientation $H\perp b$. Just for ^{51}V in this orientation the parameters were $\tau_A=5$ μs and $\tau_B=10$ μs, with $\tau_{AB}=50$ μs. Figures 3(A) and 3(B) show the temperature dependence of the spin-lattice relaxation rate for ^{7}Li and ^{51}V, respectively.

For both nuclei one finds for $T\lesssim 5$ K a strong increase of the spin-lattice relaxation rate $1/T_1(T)$ followed by a peak at
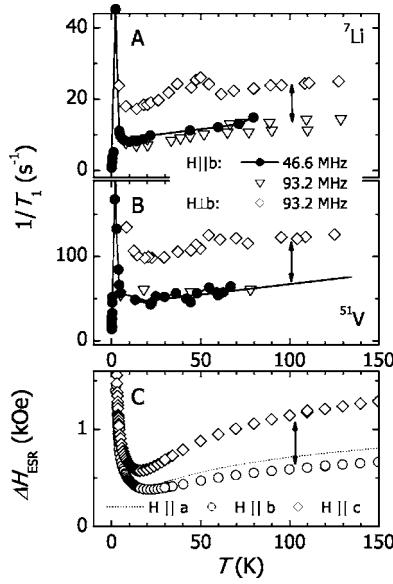
FIG. 3. Temperature dependence of the spin-lattice relaxation obtained from magnetic resonance experiments: The spin-lattice relaxation rates $1/T_1$ for ^{7}Li NMR (A) and ^{51}V NMR (B) were measured for $H\|b$ (46.6 and 93.2 MHz depicted as solid circles and open triangles, respectively) and $H\perp b$ (93.2 MHz open diamonds). The lines in (A) and (B) are drawn to guide the eye. For comparison the EPR linewidth $\Delta H_{EPR}(T)$ as measured for all three orientations of the single crystal is displayed in (C). Arrows indicate the qualitative correspondence in the orientational anisotropy for the NMR rates as well as the EPR linewidth regarding the ratio of the obtained values for orientations $H\|b$ and $H\perp b$.

$T\approx 1.3$ K, below which the rate decreases again as shown for the orientation $H\|b$ at 46.6 MHz (•). This sharp transition is indicative of a Nèel transition to a 3D-ordered antiferromagnetic state of the electronic system. To underline this feature the divergence was fitted to the following form[33] to extract a critical exponent γ and the transition temperature T_N:

$$1/T_1(T) \propto (T - T_N)^\gamma = [T - 1.3(1)]^{-0.55(3)}. \qquad (2)$$

The results are in accordance with previous determinations on powder samples.[18] The spin structure of the ordered state has recently been identified as being incommensurate, using neutron scattering.[22,23] For $T\gtrsim 10$ K, the spin-lattice relaxation rates $1/T_1(T)$ increase almost linearly with T for all measured nuclei and orientations. We recall here that in the spectra for ^{7}Li $H\|b$, two lines were observed: one for the main and one for the impurity signal, both having different relaxation rates $1/T_1(T)$. For $H\perp b$ both lines presumably overlap as they can no longer be separated in the measured spectra. Therefore, in determining the relaxation rate for $H\perp b$, there is likely to be a contribution from the extra line which could lead to the observed hump like maximum in $1/T_1(T)$ for ^{7}Li at $H\perp b$ and 93.2 MHz ($\diamond$) around $T\approx 50$ K. The different relaxation rates $1/T_1(T)$ for ^{7}Li again underline the different magnetic surroundings of the ^{7}Li nuclei contributing to the main and defect signals.
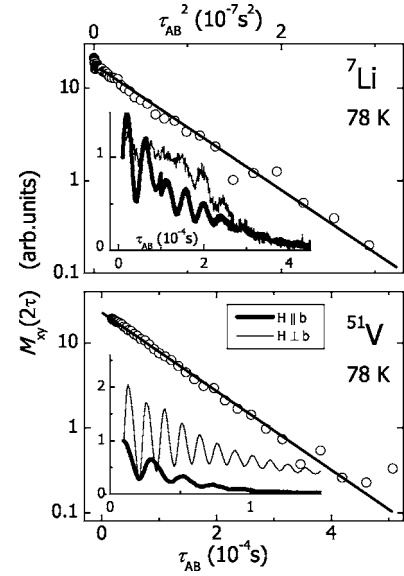

FIG. 4. Decay of the transverse magnetization $M_{xy}(2\tau)$ in the powder sample at 78 K shown for ^{7}Li (upper frame) and ^{51}V (lower frame) in the representation $M_{xy}(2\tau)$ vs τ_{AB}^2 and τ_{AB}, respectively; for details see text. The insets show the decay of $M_{xy}(2\tau)$ of single-crystalline LiCuVO$_4$ for different orientations of the crystal with respect to H.

D. Spin-spin relaxation T_2 and T_{2G}

To measure the relaxation of the transverse nuclear magnetization $M_{xy}(2\tau)$ for ^{7}Li and ^{51}V in polycrystalline powder as well as in the single crystal a spin-echo sequence was used varying the separation τ_{AB} between the pulses. The pulse parameters were $\tau_A = 4$ μs and $\tau_B = 8$ μs for polycrystalline powder and single crystal.

An example of the experimental findings in the powder sample is given in Fig. 4 on a semilogarithmic plot at $T = 78$ K, measured at 92 MHz for ^{7}Li (upper frame) and ^{51}V (lower frame). It should be noted that the signal intensity $M_{xy}(2\tau)$ is displayed semi logarithmically for both ^{51}V and ^{7}Li but as a function of τ_{AB} for ^{51}V and as a function of τ_{AB}^2 for ^{7}Li, respectively. In this representation both decays yield a straight line as indicated by the solid lines. Therefore, the decay for ^{7}Li nuclei was fitted to a Gaussian form according to

$$M_{xy}(2\tau) = M_0 \exp\left[-\frac{1}{2}\left[\frac{2\tau}{T_{2G}}\right]^2\right], \qquad (3)$$

in order to obtain the Gaussian spin-spin relaxation rate $1/T_{2G}$, whereas the one for ^{51}V nuclei was fitted to an exponential or lorentzian form $M_{xy}(2\tau) = M_0 \exp(-2\tau/T_2)$ in order to obtain the spin-spin relaxation rate $1/T_2$. These two types of transverse decays of the nuclear magnetization $M_{xy}(2\tau)$ are present as well in the single crystal. The reason for this different behavior regarding the ^{7}Li and ^{51}V decays is unclear. It might be related to the strong difference in the hyperfine interactions which revealed a tremendous anisotropy in the case of ^{7}Li and minor anisotropy for ^{51}V. This is presumably due to very different orbital overlaps along dif-

ferent paths within the LiCuVO$_4$ structure. Superimposed on the exponential decay of $M_{xy}(2\tau)$ one observes damped oscillations. For the single crystal the amplitude of these oscillations is stronger than for the powdered polycrystalline sample. As an example the respective insets for ^{7}Li and ^{51}V in Fig. 4 show the decays of the transverse magnetization $M_{xy}(2\tau)$ versus τ_{AB} as measured at 93.2 MHz and $T=5$ K for $H\parallel b$ (bold line) and $H\perp b$ (shallow line). The oscillations for ^{51}V are stronger than for ^{7}Li and show a more pronounced orientational dependence. For axial symmetry and $I=3/2$ the oscillation frequency f yields the quadrupolar splitting of the spectra, as[34–36]

$$f = \frac{\nu_Q}{2} = \frac{3eQV_{zz}}{4hI(2I-1)}(3\cos^2\theta - 1), \qquad (4)$$

where ν_Q is the quadrupolar frequency, V_{zz} is the EFG at the nuclear site, I the nuclear spin, e the electronic charge, h the Planck constant, and θ the angle between the symmetry axis of the crystal and the direction of the applied field. In case of the ^{7}Li nuclei, we obtain for the single crystal an oscillation frequency $f=21$ kHz for both orientations $H\parallel b$ and $H\perp b$ as shown in the upper inset of Fig. 4. This yields a quadrupole frequency $\nu_Q=42$ kHz in agreement with the value of 48 kHz given in Ref. 16 obtained in a polycrystalline powder sample. In the case of the ^{51}V nuclei (lower inset of Fig. 4) we obtain an oscillation frequency $f=80$ kHz for $H\perp b$ and $f=47$ kHz for $H\parallel b$, respectively. This yields a quadrupole frequency $\nu_Q=160$ kHz and $\nu_Q=94$ kHz, respectively. So f is closely related to the local point symmetry of the nucleus and therefore a sensitive probe of the local symmetry, even if the quadrupole splitting cannot be resolved in the spectra, as is the case for our ^{7}Li spectra. Indeed, the change in oscillation frequency from $H\parallel b$ to $H\perp b$ for ^{51}V corresponds roughly to the orientation-dependent splitting of the spectral lines as described above.

E. Discussion

Gaussian spin-spin relaxation in the form of Eq. (3) has been reported for the 2D system YBa$_2$Cu$_3$O$_{7-\delta}$ by Pennington *et al.*[37] Indeed the transversal decay of $M_{xy}(2\tau)$ for YBa$_2$Cu$_3$O$_{7-\delta}$ was reported to be much faster than what one might expect for a dipolar coupling of the nuclear spins. It should be mentioned that a dipolar interaction could in principle lead to Gaussian relaxation rates $1/T_{2G}$ as well, as Anersemet *et al.*[38] had reported earlier.

Pennington *et al.* suggested an indirect coupling of the Cu(2) nuclei mediated by the dynamic antiferromagnetic fluctuations of the electron spins in the CuO$_2$ planes. The time dependence of $M_{xy}(2\tau)$ within this model can be approximated by a Gaussian decay and described the experimental results for YBa$_2$Cu$_3$O$_{7-\delta}$ very well.[39] A Gaussian relaxation rate $1/T_{2G}$ was found for 1D HAFs as well.[6,40] Sachdev obtained the dependence of the NMR relaxation rates on the dynamical susceptibility $\chi(\mathbf{q},\omega)$ for 1D HAFs using spinon excitations[5] and deduced NMR relaxation rates $1/T_1(T)$ and $1/T_{2G}(T)$ in the limit $T\ll J$. For the dominant part of the electronic susceptibility at low T—namely, the

staggered susceptibility $\chi_s(\mathbf{q}=\pi,\omega)$—it has been deduced[6] for $H\parallel z$,

$$1/T_1 = [A_x^2(\pi) + A_y^2(\pi)]\frac{D}{\hbar J} = \text{const}, \qquad (5)$$

$$1/T_{2G} = \frac{A_z^2(\pi)DI}{4\hbar}\sqrt{\frac{p}{\pi k_B TJ}} \propto \frac{1}{\sqrt{T}}, \qquad (6)$$

where A_i denotes the respective hyperfine coupling constants, D is a diffusion constant, p is the natural abundance of the nucleus under investigation, and I is a constant. For the uniform part of the electronic susceptibility $\chi_u(\mathbf{q}=0,\omega)$ one expects instead

$$1/T_1 \propto T, \qquad (7)$$

$$1/T_{2G} = \text{const}. \qquad (8)$$

It was confirmed by Sandvik that with simple multiplicative, logarithmic corrections this model is still valid for $T \leqslant 0.5J/k_B$, provided that the hyperfine coupling has strong weight at $\mathbf{q}=\pi$.[41] If instead there were considerable weight for $\chi(\mathbf{q},\omega)$ at $\mathbf{q}=0$, it would be necessary to go to sufficiently low temperatures in the experiment to detect the contribution of χ_s. For Sr$_2$CuO$_3$, owing to a coupling constant $J/k_B \approx 2200$ K there was an excellent agreement between experiment and theory as shown by Takigawa *et al.*[6] and Barzykin.[7] The latter work extended Sachdev's approach and was able to express the NMR relaxation rates without free parameters.[44]

For a comparison with the Sachdev scheme we are left with the ^{7}Li results only as for ^{51}V there is no Gaussian relaxation as required within the framework of this model. The expected temperature dependence for $1/T_1(T)$ is given by Eqs. (5)–(7). The divergence of the relaxation rate $1/T_1$ due to the Nèel transition at 1.3 K makes a comparison with Sachdev's model difficult, as it overwhelms the 1D behavior at low T. A constant behavior can only be seen for $1/T_1$ around $T=5$ K after the named divergence has been subtracted (data not shown). At higher T one finds instead a linear increase as predicted for the uniform contribution to the rate $1/T_1(T)$. If we were to ignore the exact $\mathbf{q}$ dependence of the hyperfine coupling constants, we would phenomenologically assume that for $T \lesssim 5$ K the antiferromagnetic part χ_s is dominant whereas for higher T the relaxation rate is governed by the uniform part χ_u. Trying to compare the absolute numbers at $T=5$ K, following Barzykin's approach to calculate $1/T_1(T)$ for $H\parallel b$ and $H\perp b$ without free parameters,[7] we find the ratio of both relaxation rates well described by assuming for the hyperfine couplings $A_a \approx A_b$ which is reasonable from the bulk susceptibility. The derived relaxation rates are $1/T_1=33$ s^{-1} and $1/T_1=67$ s^{-1} for $H\parallel b$ and $H\perp b$, respectively, which is almost a factor of 4 off from the actual experimental findings yielding $1/T_1=6$ s^{-1} and $1/T_1=16$ s^{-1}, respectively.

As far as the spin-spin relaxation is concerned, again one is left with the ^{7}Li results for a comparison with Sachdev's model as for $M_{xy}(2\tau)$ there is no Gaussian decay for ^{51}V. To compare $1/T_{2G}$ with Eq. (6)–(8), respectively, the experi-
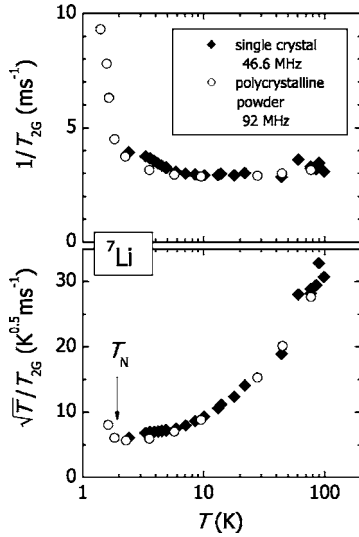
FIG. 5. Temperature dependence of $1/T_{2G}(T)$ for ^{7}Li displayed for comparison with Sachdev's model (Ref. 5); see text for details.

mental results [single crystal at 46.6 MHz $H\|b$ (♦) and polycrystalline powder at 92 MHz (○)] are depicted in Fig. 5. It should be noted that the deduced rates for polycrystalline powder and crystal coincide very well. Due to the stronger oscillations in the orientation $H\perp b$, no respective rate was derived. The representation of the temperature dependence of $1/T_{2G}$ in Fig. 5 is chosen in such a way that coincidence with the predicted temperature dependence of the NMR relaxation rates is reflected by a horizontal line. The onset of a Néel-ordered state of the electronic system at $T_N \approx 1.3$ K again restricts the temperature range for a comparison with predictions and is therefore indicated by an arrow in the figure. For $T>5$ K, the relaxation rate $1/T_{2G}(T)$ in the upper frame is nearly constant so that one would assume that for this temperature range the uniform part χ_u of the electronic susceptibility $\chi(\mathbf{q},\omega)$ dominates the spin-spin relaxation process as stated in Eq. (8). For $T_N \lesssim T \lesssim 5$ K, one finds instead that

$$\frac{\sqrt{T}}{T_{2G}} \approx \text{const} \qquad (9)$$

and one would assume that for this region the spin-spin relaxation rate $1/T_{2G}(T)$ is governed by χ_s, the antiferromagnetic part of $\chi(\mathbf{q},\omega)$ according to Eq. (6).

So, from a phenomenological point of view, one is inclined to consider a crossover from χ_s to χ_u going from low temperatures to high temperatures. To compare the actual values for $1/T_{2G}$ for $T \lesssim 5$ K with Sachdev's predictions quantitatively, following a scheme presented by Barzykin,[7] the phenomenological agreement cannot be confirmed. For $T=5$ K and $J/k_B=42$ K and the additional assumption of $A_a \approx A_b$, the model predicts a relaxation time T_{2G} in the orientation $H\|b$:

$$(T_{2G})_b = 1.91 \left(\frac{k_B T}{J}\right)^{1/2} \left(\frac{A_a^2 + A_c^2}{A_b^2}\right) T_{1b} = 0.082 \text{ s}. \quad (10)$$

This corresponds to a relaxation rate of $1/T_{2G}=0.01$ ms^{-1}, which is smaller than the experimental rate of $1/T_{2G}$

≈ 3 ms^{-1} by two orders of magnitude so that the contribution to $1/T_{2G}$ mediated by spinons is negligible. A possible reason for this is the dipolar contribution to $1/T_{2G}$ not taken into account within the framework of Sachdev's model. As a rough estimate for the dipolar contribution to $1/T_{2G}$ one would assume for a ^{7}Li distance of $r=2.9$ Å (Ref. 42):

$$\frac{1}{T_2} = \frac{\gamma^2 \hbar}{r^3} = 1.0 \text{ ms}^{-1}, \qquad (11)$$

which is indeed within the range of the experimental findings.

IV. CONCLUSION

We examined detailed NMR studies of single-crystalline LiCuVO$_4$ samples and presented results regarding the static NMR measurements: namely, ^{7}Li and ^{51}V spectra as well as respective lineshifts $K(T)$. As the deduced values for the exchange coupling constant J/k_B differ very little for both orientations ($H\|b$ and $H\perp b$), they demonstrate that the ^{7}Li and ^{51}V NMR measurements probe the microscopic properties of the electronic spin chain. Nuclear relaxation rates $1/T_1(T)$ and $1/T_{2G}(T)$ were investigated and tested against predictions of Sachdev's model where appropriate. For both nuclei ^{7}Li and ^{51}V there is an orientational dependence of the experimental relaxation rates $1/T_1(T)$. Over the whole temperature range one finds the respective rate for $H\perp b$ being twice as large as for $H\|b$. This feature resembles the orientational dependence of the EPR linewidth $\Delta H_{\text{EPR}}(T)$ as depicted in Fig. 3(C). This strong orientational dependence for the EPR measurements has been explained in the framework of an anisotropic ring exchange within the CuO$_4$ plaquettes along the Cu^{2+} chains in this compound[17] as well as for CuGeO$_3$.[43]

The NMR spectra for ^{7}Li and ^{51}V have been studied as a function of temperature and orientation of the crystal with respect to H. For all measured orientations ($H\|b$ and $H\perp b$) one finds a strong broadening of the spectra for both nuclei towards lower temperatures, which is a precursor effect of the 3D magnetic ordering of the electronic system at $T_N \approx 1.3$ K. The different orientational dependence for ^{7}Li and ^{51}V spectra is surprising. From the structure one would assume a rather axial symmetry for both positions of the nuclei, bearing in mind that the oxygen octahedron surrounding the Li$^+$ ion is elongated along the c direction and just slightly tilted. The respective values of the lineshift $K(T)$ for ^{7}Li and ^{51}V reflect very good agreement with the static susceptibility of the electronic system as is confirmed by fits to the Bonner-Fisher model yielding almost the same coupling constants J/k_B for the lineshift $K(T)$ and $\chi_{\text{bulk}}(T)$ as stated in Table I. The pronounced difference in relative lineshift as well as the strong orientational dependence for ^{7}Li compared to ^{51}V might be correlated with different paths for orbital overlap, coupling even longer distances between nuclei so that they considerably contribute to the observed lineshift.

For the relaxation rates $1/T_1(T)$ and $1/T_{2G}(T)$, the experimental findings have been compared to Sachdev's model which led to an analytic expression for the dynamic susceptibility in connection with the temperature dependence of

NMR relaxation rates $1/T_1(T)$ and $1/T_{2G}(T)$. Again regarding T_2 relaxation a Gaussian decay was found only in case for ^{7}Li. There is reasonable qualitative agreement between theory and experiment with respect to the temperature dependences. However, the calculated values can only account for 1% of the measured values. With a rough estimate for the dipolar contribution to the T_2 process, which might yield as well a Gaussian rate,[38] we are instead able to account for one-third of the experimental findings. Sachdev's model ignores any effect of dipolar interaction on the relaxation rates. This model was able to reproduce the rates for Sr_2CuO_3 excellently, so it seems likely that for systems with much lower coupling constants $J/k_B \approx 42$ K in the case of $LiCuVO_4$, dipolar contributions cannot be ignored to deduce the Gaussian rate $1/T_{2G}(T)$. We found the same discrepancy between theory and experiment for $Ba_2CuP_2O_8, Sr_2CuP_2O_8$ and $BaCuP_2O_7$.[27] Regarding the spin-lattice relaxation rate $1/T_1(T)$, it turns out that the ratio of the experimental rates for $H \| b$ and $H \perp b$ agrees with the theoretical predicted ratio. Regarding the absolute numbers, however, the predictions for $1/T_1(T)$ fail by a factor of 4 to meet the experimental findings. The temperature dependence for the EPR linewidth $\Delta H_{EPR}(T)$ for $LiCuVO_4$ shows the same qualitative behavior as the NMR spin-lattice relaxation rate $1/T_1(T)$. The former could be successfully described by using a model of symmetric anisotropic electronic exchange within a CuO_4 plaquette[17] and the same has been shown for $CuGeO_3$ earlier.[43] Of course the analysis of the 1D behavior for these materials is complicated by the onset of long-range magnetic order. But as there are very little realizations of 1D systems in nature, it is worthwhile studying their features in order to refine our knowledge of 1D systems. According to our results this might be achieved by incorporating, for example, dipolar couplings contributing to spin-spin relaxation rates and the relevant paths for orbital overlap and their significance on the lineshift as well as the scenario of anisotropic ring exchange within Cu plaquettes to account for the orientational dependence of the spin-lattice rates $1/T_1(T)$ resembling the behavior of the EPR linewidth.

*Present address: Bio-Medical Physics & Bio-Engineering, University of Aberdeen, Foresterhill, AB25 2ZD, Aberdeen, Scotland, UK.

[1] I. Affleck, in *1988 Les Houches Lectures*, edited by E. Brezin and J. Zinn-Justin (North-Holland, Amsterdam, 1990).

[2] M. Hase, I. Terasaki, and K. Uchinokura, Phys. Rev. Lett. **70**, 3651 (1993).

[3] E. Ehrenfreund, E. F. Rybaczewski, A. F. Garito, A. J. Heeger, and P. Pincus, Phys. Rev. B **7**, 421 (1973).

[4] A. J. Millis, H. Monien, and D. Pines, Phys. Rev. B **42**, 167 (1990).

[5] S. Sachdev, Phys. Rev. B **50**, 13006 (1994).

[6] M. Takigawa, N. Motoyama, H. Eisaki, and S. Uchida, Phys. Rev. Lett. **76**, 4612 (1996).

[7] V. Barzykin, Phys. Rev. B **63**, 140412(R) (2001).

[8] N. Motoyama, H. Eisaki, and S. Uchida, Phys. Rev. Lett. **76**, 3212 (1996).

[9] A. F. Corsmit and G. Blasse, Chem. Phys. Lett. **20**, 347 (1973).

[10] M. Lafontaine, M. Leblanc, and G. Ferey, Acta Crystallogr., Sect. C: Cryst. Struct. Commun. **45**, 1205 (1989).

[11] G. Blasse, J. Phys. Chem. Solids **27**, 612 (1966).

[12] A. N. Vasil'ev, JETP Lett. **69**, 876 (1999).

[13] C. González, M. Gaitan, M. L. Lopez, M. L. Veiga, R. Saezpuche, and C. Pico, J. Mater. Sci. **29**, 3458 (1994).

[14] M. Yamaguchi, T. Furuta, and M. Ishikawa, J. Phys. Soc. Jpn. **65**, 2998 (1996).

[15] R. Kanno, Y. Takeda, M. Hasegawa, Y. Kawamoto, and O. Yamamoto, J. Solid State Chem. **94**(2), 319 (1991).

[16] H. Saji, J. Phys. Soc. Jpn. **33**, 671 (1972).

[17] H.-A. Krug von Nidda, L. E. Svistov, M. V. Eremin, R. M. Eremina, A. Loidl, V. Kataev, A. Validov, A. Prokofiev, and W. Aßmus, Phys. Rev. B **65**, 134445 (2002).

[18] C. Kegler, N. Büttgen, H.-A. Krug von Nidda, A. Krimmel, L. Svistov, B. I. Kochelaev, A. Loidl, A. Prokofiev, and W. Aßmus, Eur. Phys. J. B **22**, 321 (2001).

[19] A. N. Vasil'ev, L. A. Ponomarenko, H. Manaka, I. Yamada, M. Isobe, and Y. Ueda, Phys. Rev. B **64**, 024419 (2001).

[20] T. Tanaka, H. Ishida, M. Matsumoto, and S. Wada, J. Phys. Soc. Jpn. **71**, 308 (2002).

[21] A. V. Prokofiev, D. Wichert, and W. Aßmus, J. Cryst. Growth **220**, 354 (2000).

[22] B. J. Gibson, R. K. Kremer, A. V. Prokofiev, W. Aßmus, and G. J. McIntyre, Physica B **350**, e253 (2004).

[23] M. Enderle, C. Muherjee, B. Fåk, R. K. Kremer, J.-M. Broto, H. Rosner, S.-L. Drechsler, J. Richter, J. Malek, A. Prokofiev, W. Aßmus, S. Pujol, J.-L. Raggazzoni, H. Rakoto, M. Rheinstädter, and H. M. Rønnow, Europhys. Lett. **70**, 237 (2005).

[24] L. S. Parfen'eva, A. I. Shelykh, I. A. Smirnov, A. V. Prokof'ev, W. Aßmus, H. Misiorek, J. Mucha, A. Jezowski, and I. G. Vasil'eva, Phys. Solid State **45**, 2093 (2003).

[25] L. S. Parfen'eva, I. A. Smirnov, H. Misiorek, J. Mucha, A. Jezowski, A. V. Prokof'ev, and W. Aßmus, Phys. Solid State **46**, 357 (2004).

[26] B. Gorshunov, P. Haas, M. Dressel, V. I. Torgashev, V. B. Shirokov, A. Prokofiev, and W. Aßmus Eur. Phys. J. B **23**, 427 (2001).

[27] R. Nath, A. V. Mahajan, N. Büttgen, C. Kegler, and A. Loidl, Phys. Rev. B **71**, 174436 (2005).

[28] E. D. Jones, Phys. Rev. **151**, 315 (1966).

[29] J. C. Bonner and M. E. Fisher, Phys. Rev. **135**, A640 (1964).

[30] W. E. Estes, D. P. Gavel, and D. Hodgson, Inorg. Chem. **17**, 1415 (1978).

[31] A. Clogston and V. Jaccarino, Phys. Rev. **121**, 1357 (1961).

[32] A. M. Clogston, V. Jaccarino, and Y. Yafet, Phys. Rev. **134**, A650 (1964).

[33] V. Jaccarino, in *Magnetism: A Treatise on Modern Theory and Materials*, Vol. 2A of Magnetism, edited by G. T. Rado and H. Suhl (Academic Press, San Diego, 1965), Chap. 5, p. 307.

[34] H. Abe, H. Yasuoka, and A. Hirai, J. Phys. Soc. Jpn. **21**, 77 (1966).

[35] N. Shamir, N Kaplan, and J. H. Wernick, J. Phys. (Paris), Colloq. **32**, C1-902 (1971).

[36] E. Dormann, in *Advances in Solid State Physics, Festkörperprobleme XII* (Pergamon Vieweg, Weinheim, 1972).

[37] C. H. Pennington, D. J. Durand, C. P. Slichter, J. P. Rice, E. D. Bukowski, and D. M. Ginsberg, Phys. Rev. B **39**, R274 (1989).

[38] J. P. Anersemet, C. P. Slichter, and J. H. Sinfelt, J. Chem. Phys. **88**, 5963 (1988).

[39] C. H. Pennington and C. P. Slichter, Phys. Rev. Lett. **66**, 381 (1991).

[40] M. Itoh, M. Sugahara, T. Yamauchi, and Y. Ueda, Phys. Rev. B **54**, R9631 (1996).

[41] A. W. Sandvik, Phys. Rev. B **52**, R9831 (1995).

[42] C. P. Slichter, *Principles of Magnetic Resonance* (Springer, Berlin, 1990).

[43] R. M. Eremina, M. V. Eremin, V. N. Glazkov, H.-A. Krug von Nidda, and A. Loidl, Phys. Rev. B **68**, 014417 (2003).

[44] He showed that for the experimental relaxation rates $1/T_1$ (T) and $1/T_{2G}$ (T) the relation $(T_{2G})_b = 1.91(k_B T/J)^{1/2}[(A_a^2 + A_c^2)/A_b^2]T_{1b}$, with A_a, A_b and A_c being the hyperfine constants for $H \| a$, $H \| b$, and $H \| c$, respectively.